Evaluating a satellite-derived global infrared land surface emissivity data set for use in radiative transfer modeling

Ronald L. Vogel,[1] Quanhua Liu,[2] Yong Han,[3] and Fuzhong Weng[3]

Received 9 July 2010; revised 19 January 2011; accepted 7 February 2011; published 19 April 2011.

[1] Radiative transfer models rely on accurate atmospheric and surface conditions for simulating top-of-atmosphere satellite radiance. Over land surfaces, emissivity is especially important for simulating surface-sensitive channels, owing to its spatial and temporal variability. In this study, the University of Wisconsin Global Infrared Land Surface Emissivity Database (UWIREMIS) has been evaluated in the Community Radiative Transfer Model (CRTM). Radiative transfer simulations of top-of-atmosphere Spinning Enhanced Visible and Infrared Imager (SEVIRI) brightness temperature have been compared to actual SEVIRI brightness temperature observations for 30 May 2010 at 0000 UTC, using both the UWIREMIS and the current internal CRTM emissivity data sets as surface input to CRTM. When using UWIREMIS, a brightness temperature bias of −0.85 K for the SEVIRI 8.7 μm channel is due in part to excellent characterization of the emissivity spectrum for bare ground surfaces in this spectral region, compared to a bias of −2.55 K when using the existing CRTM emissivity. Additionally, UWIREMIS has been compared to the North American ASTER Land Surface Emissivity Database (NAALSED), a validated land surface emissivity data set, and low emissivity biases of 0.004 (summer) and 0.007 (winter) indicate UWIREMIS accuracy for the NAALSED spatial domain and the spectral region of the Advanced Spaceborne Thermal Emission and Reflection Radiometer (ASTER) channels. With its high spectral and high spatial resolution, UWIREMIS is well suited for providing the infrared surface emissivity contribution to radiative transfer models. Additional work will be needed to assess UWIREMIS for more spectral regions, surface types, and time periods.

Citation: Vogel, R. L., Q. Liu, Y. Han, and F. Weng (2011), Evaluating a satellite-derived global infrared land surface emissivity data set for use in radiative transfer modeling, *J. Geophys. Res.*, *116*, D08105, doi:10.1029/2010JD014679.

1. Introduction

[2] The radiative transfer community requires multifunctional, rapid and accurate radiance and radiance gradient models for satellite data assimilation, sensor design and specification, calibration and validation of remote sensing data, and other research activities. The accurate and fast radiative transfer models require surface conditions, including surface emissivity, for simulating top-of-atmosphere satellite observations. For surface-sensitive window channels, the emissivity is especially necessary for accurately estimating satellite radiance. The estimation of satellite radiance is a key component of assimilating satellite data into numerical weather prediction (NWP) models. In addition, surface emissivity is crucial for estimating surface temperature from satellite measurements [*Yu et al.*, 2008], retrieval of atmospheric moisture and temperature profiles from satellites [*Seemann et al.*, 2008], and studies of the Earth's surface-atmosphere system such as surface energy balance and climate modeling [*Zhou et al.*, 2003]. The accuracy of the emissivity is important for accurate retrievals. For example, an emissivity error of 0.005 can be shown to correspond to a surface temperature error of 0.3 K [*Hulley and Hook*, 2009].

[3] Emissivity is defined as the ratio of the emitted radiant flux of a material at a given temperature to the emitted radiant flux of a blackbody at the same temperature. Thus, it is a fractional unitless quantity and is an inherent property of the material. From a practical perspective, emissivity can be conceptualized as the "emitting ability" of a material [*Lillesand et al.*, 2004]: the higher the fraction, the better the material is at absorbing and reemitting the energy incident upon it. Also, emissivity varies spectrally for a material across the electromagnetic spectrum; the shape of the spectrum depends on the properties of the surface and can be used to identify the mineral composition of the underlying material.

[4] For land surfaces, emissivity is highly variable owing to the many materials that make up the Earth's land surface. Thermal infrared (8–12 μm) land surface emissivity varies

[1]SM Resources Corporation, Lanham, Maryland, USA.
[2]Perot Systems Government Services, Fairfax, Virginia, USA.
[3]Center for Satellite Applications and Research, NOAA, NESDIS, Camp Springs, Maryland, USA.

Copyright 2011 by the American Geophysical Union.
0148-0227/11/2010JD014679

from ~0.65 to very close to 1.0 [*Hulley and Hook*, 2009]. Vegetated areas typically have high emissivity (0.9–1.0) and exhibit variation seasonally [*Ruston et al.*, 2008]. Exposed ground and desert emissivities on the other hand are lower and more variable, particularly for the spectral region 8.0–10.0 μm, owing to the presence of quartz in many geologic surfaces [*Salisbury and D'Aria*, 1992]. In this paper, we consider surface emissivity in the infrared spectral range of 3.5–14.0 μm.

[5] The Community Radiative Transfer Model (CRTM) [*Han et al.*, 2005] is the radiative transfer model used at NOAA's National Centers for Environmental Prediction (NCEP) for assimilation of satellite data into operational NWP models. The CRTM achieves an accuracy better than 0.1 K in comparison to line-by-line transmittance calculations for infrared and microwave sounding channels and all atmospheric conditions [*Chen et al.*, 2010]. It is a fundamental model in radiance simulation and in data assimilation and is used for hurricane forecasting [*Liu and Weng*, 2006] and for monitoring satellite infrared clear-sky radiance over oceans [*Liang et al.*, 2009].

[6] The CRTM's current infrared land surface emissivity data set was utilized in the algorithm development program of the National Polar-orbiting Operational Environmental Satellite System (NPOESS) and was adopted for use in CRTM. It is referred to here as the NPOESS emissivity data set, or simply NPOESS. It consists of one reflectance spectrum for each of 24 surface types (24 reflectance spectra total) [*Han et al.*, 2005], and emissivity is calculated as one minus reflectance under the assumption of a Lambertian surface in the infrared spectral region [*Salisbury et al.*, 1994]. The spectra lack any variation in the time dimension; that is, there is no seasonal emissivity variation to account for seasonal cycles. Furthermore, the spectral variation for the bare ground surface types inadequately captures the high variability in soil and desert emissivity. Additionally, the reliance on surface type classification oversimplifies the spatial variation in surface emissivity, which varies over very small spatial scales, and surface types can also introduce step discontinuities in emissivity spatially. Moreover, variation in soil moisture is not taken into account, which can increase emissivity by up to 16%, especially in sandy soil in the 8.2–9.2 μm range [*Mira et al.*, 2007].

[7] Given the limitations of the current emissivity data set used in CRTM, we explore the possibility of using the University of Wisconsin Global Infrared Land Surface Emissivity Database (UWIREMIS) as an alternative emissivity data set for radiative transfer modeling. The following evaluation includes a description of the various data sets employed, a comparison of satellite observations from the Spinning Enhanced Visible and Infrared Imager (SEVIRI) to CRTM satellite simulations of SEVIRI to judge the efficacy of the two emissivity data sets, an assessment of UWIREMIS against a validated emissivity data set from the Advanced Spaceborne Thermal Emission and Reflection Radiometer (ASTER), and discussion of the results.

2. Data Set Backgrounds and Radiative Transfer Model Sensitivity

[8] The data sets utilized in this study are described briefly below. Three emissivity data sets are used: NPOESS, UWIREMIS, and the North American ASTER Land Surface Emissivity Database (NAALSED). The NPOESS and UWIREMIS emissivity data sets are compared to each other, whereas the NAALSED emissivity data set is used for assessing emissivity accuracy. In addition, satellite multispectral data from SEVIRI are used to compare radiative transfer simulation results from the CRTM to actual satellite observations. As such, an assessment of CRTM's sensitivity to uncertainty in atmospheric and surface inputs is provided for the SEVIRI channels and SEVIRI scene used in this study.

2.1. NPOESS

[9] NPOESS is the current emissivity data set included in the CRTM [*Han et al.*, 2005]. It consists of one reflectance spectrum for each of 24 surface types. The spectral range is 0.2–15.0 μm, and the spectral resolution varies from 0.025 μm to 1.0 μm, depending on spectral region. Knowledge of the surface type is required in order to determine an emissivity value from the 24 spectra. Since most users derive surface inputs to CRTM from their own applications, which most likely have their own surface classification scheme, it is necessary to match surface type classes between the user's classification scheme and the CRTM classification scheme. Such matching of surface classification schemes assumes that the emissivity characteristics of a particular surface are comparable between classification schemes; that is, users must be careful to match emissivity characteristics of a class and not just rely on similar names between classification schemes. Figure 1 depicts the Simple Biosphere-1 (SiB-1) classification scheme of *Dorman and Sellers* [1989] used operationally in the NCEP Global Data Assimilation System [*Ek et al.*, 2003]. Figure 2a displays the NPOESS emissivity spectra as matched to the SiB-1classification scheme. In comparison, Figure 2b displays the UWIREMIS averaged globally for the SiB-1 classification scheme. Comparison of Figures 2a and 2b illustrates the inadequacy of bare ground emissivity information in the NPOESS emissivity data set as matched to the SiB-1 classification scheme. Note in particular the wavelengths 8–10 μm where bare ground surfaces are particularly variable. UWIREMIS reveals distinctions in emissivity characteristics (the quartz *reststrahlen* feature) for the three surface types that cover desert areas: bare soil, broadleaf shrub with bare soil, and broadleaf shrub with groundcover. However, these spectral features are lacking in the NPOESS emissivity data set for the same surface types. As stated earlier, other limitations of the NPOESS emissivity data set are the lack of temporal variation in emissivity for seasonal changes and the lack of variation to account for soil moisture.

2.2. UWIREMIS

[10] UWIREMIS is a monthly emissivity data set derived from emissivity retrievals from the Moderate Resolution Imaging Spectroradiometer (MODIS) on the NASA Aqua satellite [*Seemann et al.*, 2008]. The MODIS emissivities are retrieved for six infrared channels using the Day-Night Land Surface Temperature and Emissivity algorithm [*Wan and Li*, 1997] and composited monthly on a 0.05° spatial grid. UWIREMIS uses a fitting approach to estimate emissivity at 10 hinge points (inflection points in a generalized emissivity

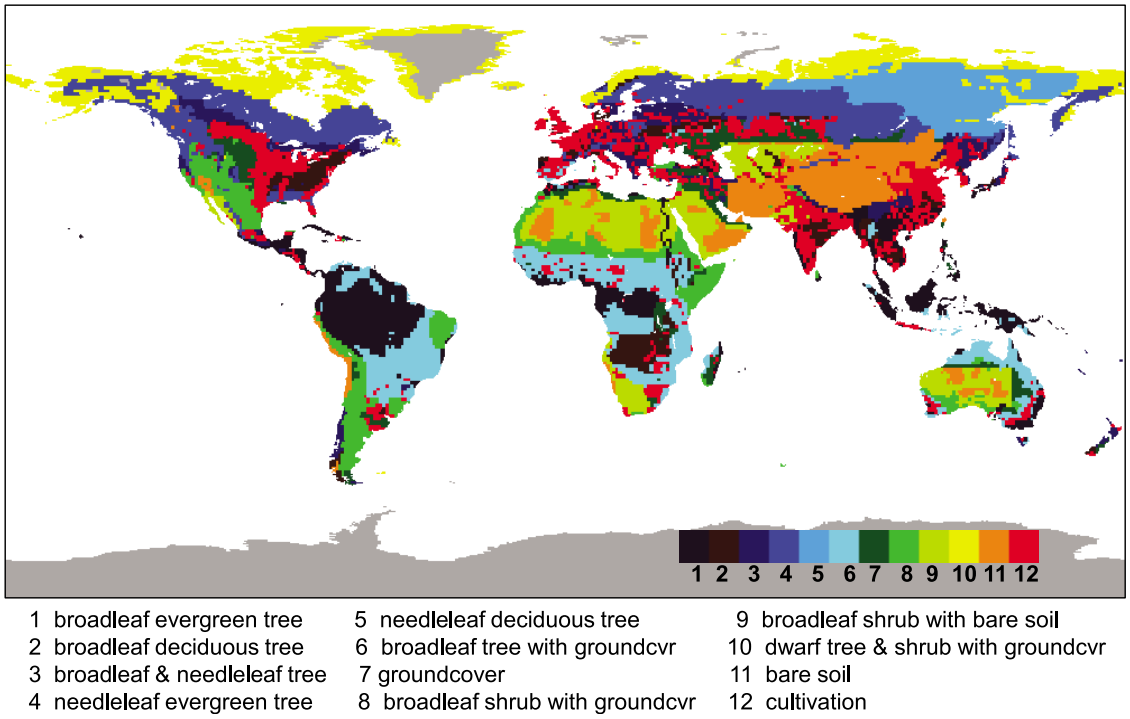

Figure 1. The Simple Biosphere-1 (SiB-1) surface classification scheme used in the National Centers for Environmental Prediction Global Data Assimilation System. Ocean (white) and ice (gray) are also given in SiB-1 but are not germane to this study.

spectrum) based on the MODIS-retrieved emissivity values at the six channels and knowledge of the expected emissivity spectrum from laboratory measurements. Thus, while the MODIS-retrieved emissivities themselves cannot be interpolated between the instrument's channels, the UWIREMIS emissivities can be interpolated between the hinge points, making them useful for applications such as data assimilation that involve multiple sensors. The 10 hinge points are 3.6, 4.3, 5.0, 5.8, 7.6, 8.3, 9.3, 10.8, 12.1, and 14.3 μm. In addition, using principal components regression and eigenvectors from 123 laboratory-measured emissivity spectra, a high spectral resolution emissivity data set at 416 spectral points can be calculated from the 10 hinge points [*Borbas et al.*, 2007]. The laboratory-measured spectra are of high resolution and obtained from the MODIS Emissivity Library at University of California, Santa Barbara, and the ASTER Spectral Library [*Baldridge et al.*, 2009]. Thus, UWIREMIS contains a spectrum of monthly averaged emissivity at 416 spectral points at each latitude-longitude location on a 0.05° spatial resolution grid. The 416 spectral points are in wave numbers and have a spectral resolution of 5.0 cm^{-1} from 699.3 cm^{-1} to 2774.3 cm^{-1}, that is, 14.3–3.6 μm.

[11] In an earlier evaluation of UWIREMIS, *Collard* [2009] observed a large year-to-year variability in emissivity for the same month in different years. While this may be due to interannual differences in the atmosphere, soil moisture (e.g., drought), or land cover, the possibility of emissivity algorithm error or hinge-point fitting error cannot be overlooked. Consequently, we average the monthly UWIREMIS emissivity values for the years 2003–2006 to create a monthly climatology of emissivity.

[12] Figure 3 displays a spatial comparison of NPOESS and UWIREMIS at four surface-sensing channels (corresponding to the four infrared surface-sensing channels on SEVIRI). The UWIREMIS values are averaged for the month of May for the years 2003–2006. Differences are apparent, notably at 3.9 and 8.7 μm. At 3.9 μm, NPOESS emissivity is much lower in the northern hemisphere with the exception of the Sahara Desert for which UWIREMIS has much lower emissivity. At 8.7 μm, UWIREMIS exhibits much lower emissivity than NPOESS for all major desert areas globally, indicative of the low spectral feature seen in Figure 2b in the 8–10 μm region.

[13] Figure 3 also demonstrates how the deserts of the Earth vary in their emissivity characteristics owing to differing mineralogy and presence/absence of vegetation. UWIREMIS at 3.9, 8.7 and 10.8 μm all reveal that the Sahara Desert exhibits much lower emissivity compared to the deserts of western North America or central Asia–western China. This difference among deserts exemplifies the shortcoming of the classification approach: use of a single desert class will not characterize the very large differences in emissivity between these three major desert regions.

[14] The high emissivity values of Greenland and Antarctica can also be seen in Figure 3. This feature is due to the high emissivity of ice at all infrared wavelengths.

2.3. NAALSED

[15] The North American ASTER Land Surface Emissivity Database (NAALSED) is an emissivity composite of scenes from the ASTER instrument on the NASA Terra satellite for the life of the ASTER mission [*Hulley et al.*,

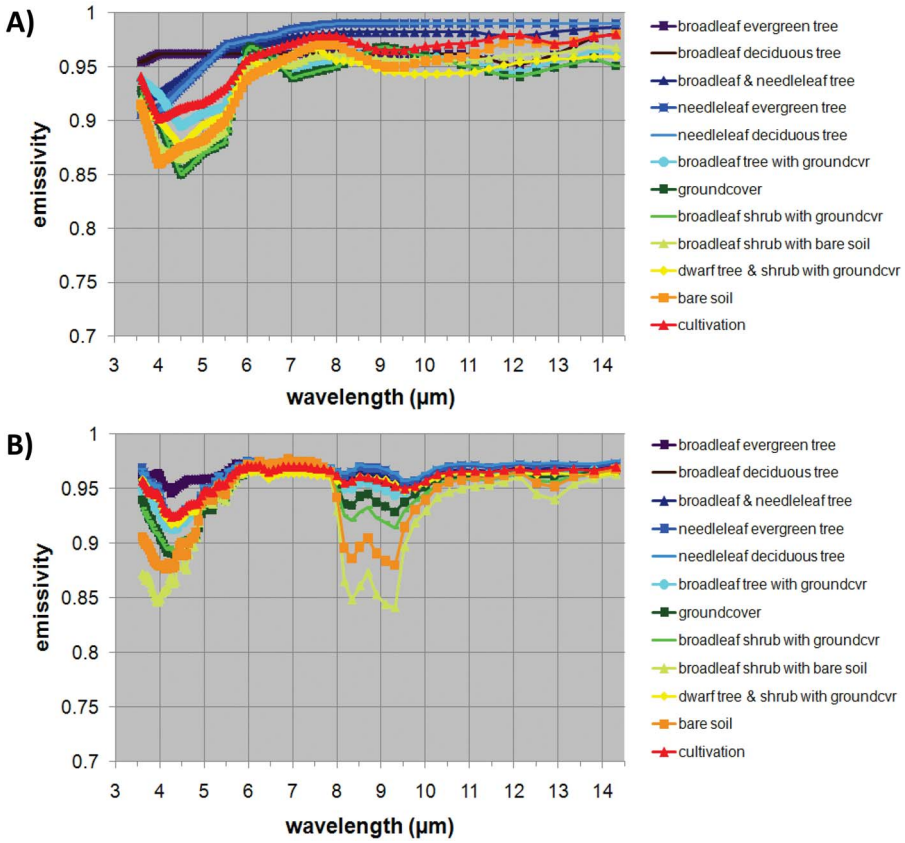

Figure 2. Emissivity spectra by surface class for (a) the NPOESS emissivity data set and (b) the UWIREMIS data set. The NPOESS spectra are matched to the SiB-1 surface classification scheme. The UWIREMIS spectra are for the month of July 2008 and were determined by averaging globally for each of the SiB-1 surface classes. The legend on the right lists the SiB-1 classes.

2008; *Hulley and Hook*, 2009]. The surface emissivity is retrieved from ASTER observations using the Temperature Emissivity Separation algorithm [*Gillespie et al.*, 1998] for the five ASTER thermal infrared channels at 8.3, 8.7, 9.1, 10.6, and 11.3 μm. The emissivity values are composited for each channel for clear-sky pixels on a 100 m grid over the contiguous United States (ASTER spatial resolution is 90 m). Two seasonal mean data sets are available: a summertime composite of all ASTER scenes for the months July, August and September for the years 2000–2008, and a wintertime composite of all ASTER scenes for the months January, February and March for the years 2000–2008. NAALSED has been produced on spatial grids of resolutions 100 m, 1 km, 5 km, and 50 km.

[16] Figure 4a shows the NAALSED summer mean emissivity for the 8.7 μm channel. Missing data are expected to be collected by the ASTER instrument in forthcoming years and added to the NAALSED summer and winter databases. NAALSED has been validated using desert in situ sites in the western United States [*Hulley et al.*, 2009]. The mean difference for all nine in situ sites and all five channels was found to be 0.016, which represents approximately a 1 K error in land surface temperature retrieval from satellite measurements. As a comparison of NAALSED with UWIREMIS, Figure 4b shows the UWIREMIS emissivity for the NAALSED region and averaged for the months July, August, and September over the years 2003–2006. The high spectral resolution UWIREMIS was convolved with the ASTER 8.7 μm channel spectral response function. There is a strong qualitative similarity between NAALSED and UWIREMIS both in the magnitude of emissivity values and in geophysical emissivity features.

[17] This study does not consider the 8.3 μm channel in the NAALSED database owing to its proximity to water vapor absorption bands. The emissivity values at this wavelength are less accurate [*Gillespie et al.*, 1998].

2.4. SEVIRI

[18] In this study, we compare satellite observations from SEVIRI with CRTM top-of-atmosphere simulations of SEVIRI. The SEVIRI instrument on the Meteosat-9 geostationary satellite is positioned at 0° latitude and 0° longitude at an altitude of 35,800 km. A multispectral imaging instrument, SEVIRI images the full disk of the Earth every 15 min in 12 spectral channels [*Aminou et al.*, 1997], eight of which are infrared channels. Of the infrared channels, this study utilizes the four surface-sensing channels, all at 3 km spatial resolution. The central wavelengths of the surface-sensing channels are 3.9, 8.7, 10.8, and 12.0 μm. The noise equivalent delta temperature (NEDT) for the four surface-sensing channels is 0.24, 0.15, 0.13, and 0.21 K, respectively. An example of SEVIRI brightness temperature for the day and time used in this study (30 May 2010 at

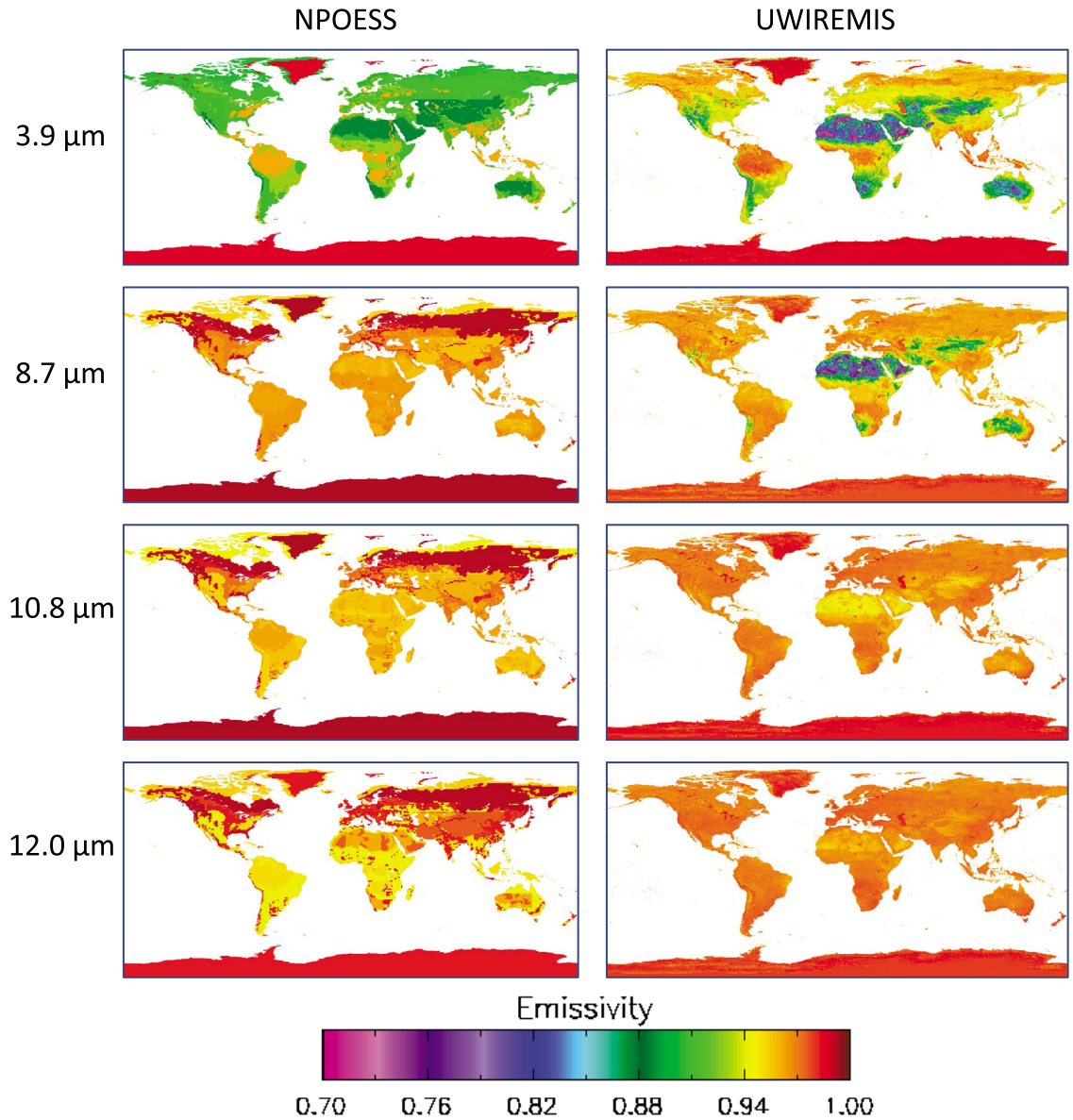

Figure 3. Emissivity maps of (left) the NPOESS emissivity data set and (right) the UWIREMIS data set for the infrared surface-sensing channels on SEVIRI. NPOESS values are mapped to the SiB-1 surface classification scheme. UWIREMIS values are the monthly climatology for May (2003–2006 average).

0000 UTC) for the 10.8 μm channel is shown in Figure 5. Low values are clouds.

2.5. CRTM Sensitivity to Atmospheric and Surface Inputs

[19] CRTM simulated brightness temperature is sensitive to uncertainties in its atmospheric and surface inputs. We analyzed the sensitivity of CRTM for simulating the surface-sensitive infrared SEVIRI channels for 30 May 2010 at 0000 UTC. For atmospheric and surface inputs, we used atmospheric profiles of temperature, water vapor, ozone and cloud water content from the NCEP Global Data Assimilation System (GDAS) analysis, surface temperature also from NCEP GDAS analysis, and surface emissivity from UWIREMIS. The atmospheric temperature, water vapor, surface temperature, and surface emissivity were each perturbed in a separate run of CRTM, brightness temperature was simulated, and the simulation was compared with a nonperturbed reference simulation. Perturbations were random with a uniform distribution such that the maximum perturbation (in the negative direction) was −2 K for the atmospheric temperature profile (applied to all profile layers), −10% for the water vapor profile (applied to all layers), −2 K for the surface temperature, and −0.02 for the surface emissivity. Only negative perturbations were used to avoid exceeding reasonable water vapor and emissivity values if positive perturbations had been used, and to avoid canceling the perturbation in the radiative transfer calculation if both positive and negative perturbations had been used (e.g., an increase in one atmospheric layer may be compensated by a decrease in another layer for the same atmospheric profile). Clouds, clear ocean, and clear land were all included in the

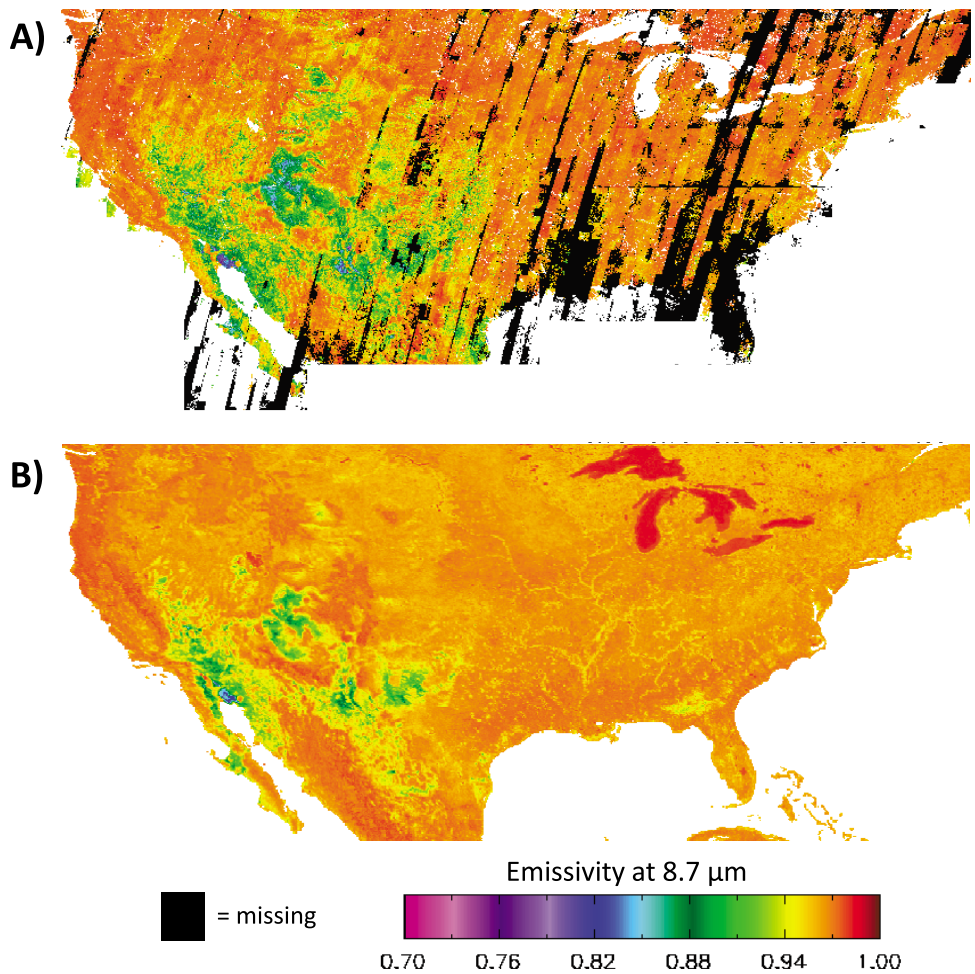

Figure 4. Comparison of (a) NAALSED emissivity and (b) UWIREMIS emissivity for the ASTER 8.7 μm channel. NAALSED is composited for the months of July, August, and September over the period 2000–2008. UWIREMIS is averaged for the months of July, August, and September over the period 2003–2006 and convolved for the 8.7 μm ASTER channel.

simulation. Since the entire SEVIRI full disk view was simulated, the profiles include moist (tropical), dry (desert), hot (equatorial), and cool (high-latitude) conditions. The CRTM's brightness temperature sensitivity for clear land surface for the four surface-sensing infrared channels, given in root mean square error, was 0.3–0.7 K for the −2 K atmospheric temperature perturbation, 0.1–0.4 K for the −10% water vapor perturbation, 0.5–0.9 K for the −2 K surface temperature perturbation, and 0.2–0.3 K for the −0.02 surface emissivity perturbation. Sensitivity for the following cases is given in Table 1: cloud, clear ocean, clear land, and clear land in the Sahara region.

3. Method

[20] Evaluation of the emissivity data sets was performed by comparing CRTM top-of-atmosphere brightness temperature simulations, run with the two emissivity data sets, to actual SEVIRI satellite observations. The UWIREMIS was then further evaluated for accuracy by comparison with NAALSED.

3.1. Comparison of CRTM Simulations to Satellite Observations

[21] In order to evaluate the effectiveness of surface emissivity in contributing to the modeled top-of-atmosphere satellite simulations, the CRTM was run with both the NPOESS and UWIREMIS emissivity data sets, and the resulting top-of-atmosphere brightness temperature simulations were compared to actual satellite-observed brightness temperature of the SEVIRI instrument. A SEVIRI full-disk image of 30 May 2010 at time 0000 UTC was selected owing to low cloud coverage at that time over most of the full disk view. All four infrared surface-sensing channels were simulated with CRTM and compared to SEVIRI observations.

[22] Analysis fields from the European Centre for Medium-Range Weather Forecasts (ECMWF) were used as atmospheric and surface input to CRTM [*Persson and Grazzini*, 2007]. Analysis fields for the same day as the SEVIRI observations and at cycle time 0000 UTC were used. It is important to note that the SEVIRI infrared surface-sensing channels were not assimilated into the analysis fields, so the analysis inputs to CRTM are uncor-

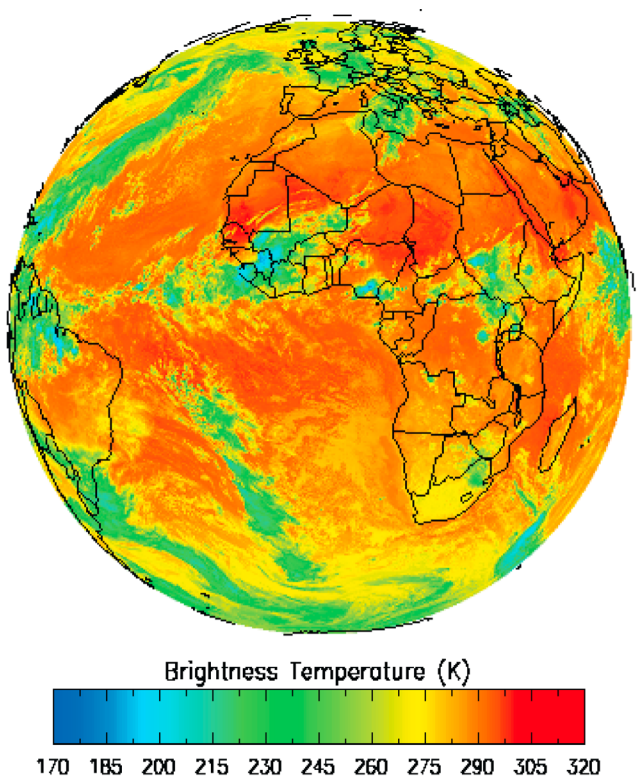

Figure 5. SEVIRI brightness temperature (K) at 10.8 μm for 30 May 2010 at 0000 UTC.

related with the SEVIRI observations in this comparison. The ECMWF atmospheric profile fields had 91 vertical layers on a global grid of 0.25° spatial resolution. Profiles of temperature, pressure, humidity, and ozone were input into CRTM, as was ECMWF surface temperature on the same global grid. Surface types for each grid point were obtained from the MODIS land cover classification data product [*Friedl et al.*, 2002] using the International Geosphere-Biosphere Program (IGBP) classification scheme and matched to the CRTM's NPOESS surface types in order to select the emissivity spectrum from the NPOESS emissivity data set (the NPOESS surface types used in the SiB-1-to-NPOESS matching are the same NPOESS surface types used in the IGBP-to-NPOESS matching). The four analysis grid points surrounding a satellite pixel were bilinearly interpolated to the satellite pixel location. Ocean pixels were excluded using a land-ocean mask. Clouds were masked with an infrared multichannel cloud property algorithm using the SEVIRI infrared channels and a cloudiness threshold to identify cloudy regions (not a standard SEVIRI cloud mask product). Coastal pixels were not excluded from this evaluation.

[23] After simulating top-of-atmosphere brightness temperature with CRTM for the two emissivity cases: first with NPOESS and then with UWIREMIS, the two simulation cases were each compared to SEVIRI observed brightness temperature for the four surface-sensing channels for cloud-free, land pixels. Observation minus simulation differences, mean difference (bias), and root mean square error (RMSE) were calculated.

Table 1. Sensitivity in RMSE of CRTM Simulated Brightness Temperature to Uncertainty in Atmospheric Profiles and Surface Conditions for the Four Infrared Surface-Sensing Channels of SEVIRI on 30 May 2010 at 0000 UTC[a]

Channel (μm)	RMSE (K) Cloud (44%)	Clear Water (45%)	Clear Land (11%)	Clear Land, 10°N–30°N, −30°W–+30°E (2%)
	−2 K Perturbation for Atmospheric Temperature Profile			
3.9	0.632	0.244	0.276	0.161
8.7	0.826	0.375	0.459	0.377
10.8	0.868	0.449	0.541	0.440
12.0	0.899	0.545	0.670	0.580
	−10% Perturbation for Atmospheric Water Vapor Profile			
3.9	0.011	0.126	0.139	0.023
8.7	0.069	0.162	0.198	0.166
10.8	0.096	0.232	0.283	0.294
12.0	0.119	0.268	0.366	0.417
	−2 K Perturbation for Surface Temperature			
3.9	0.402	0.673	0.854	0.913
8.7	0.190	0.509	0.664	0.719
10.8	0.172	0.496	0.660	0.768
12.0	0.122	0.388	0.545	0.641
	−0.02 Perturbation for Surface Emissivity			
3.9	0.098	0.144	0.185	0.235
8.7	0.060	0.188	0.250	0.322
10.8	0.054	0.221	0.305	0.388
12.0	0.044	0.170	0.247	0.306

[a]Atmospheric profiles and surface temperature are from National Centers for Environmental Prediction Global Data Assimilation System, and surface emissivity is from UWIREMIS. Scene percentage is percentage of total scene.

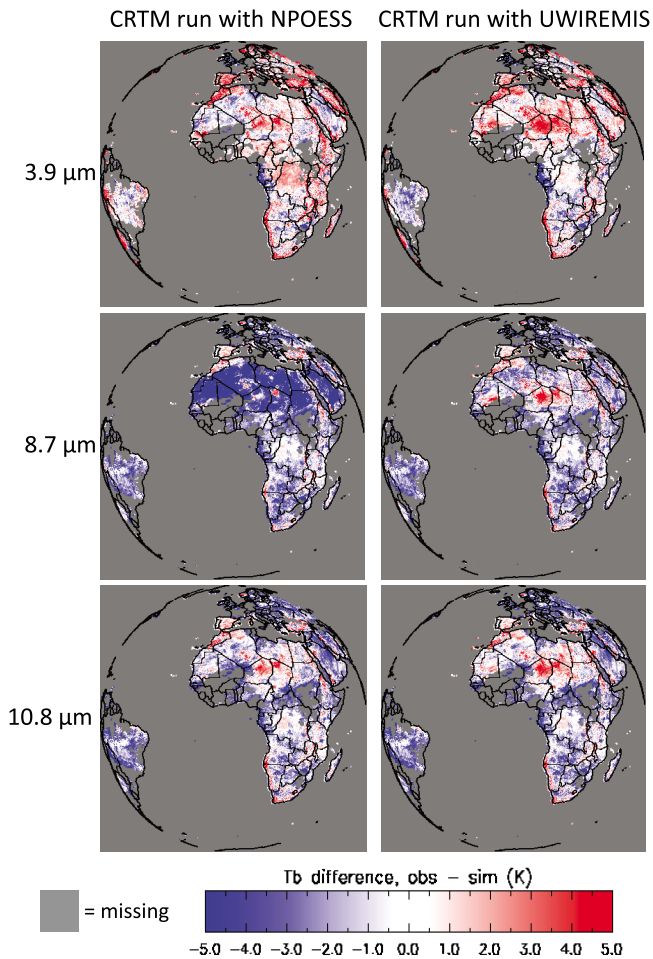

Figure 6. Brightness temperature difference (K) between SEVIRI observations and CRTM simulations (observations minus simulations) at three SEVIRI infrared surface-sensing channels for 30 May 2010 at 0000 UTC: (left) CRTM run with NPOESS emissivity and (right) CRTM run with UWIREMIS emissivity.

[24] A nighttime SEVIRI scene was chosen for this study because daytime CRTM simulations over land regions are impacted by solar radiation and are not corrected for land BRDF effects.

3.2. Intercomparison With NAALSED

[25] Since NAALSED has been validated against desert in situ emissivity measurements, it is possible to assess the accuracy of other emissivity data sets against NAALSED. Given its high spatial resolution and good accuracy, other data sets at coarser spatial resolution can be compared to NAALSED by downscaling NAALSED to the coarser spatial resolution.

[26] In this comparison, we estimated the bias of UWIREMIS to NAALSED. In doing so, the monthly UWIREMIS data were averaged by month for the 4 year period 2003–2006, producing a month-by-month 4 year climatological average. The 4 year monthly averages were then averaged for the summer and winter seasons: the July, August and September 4 year averages were averaged to create a summer seasonal emissivity, and the January, February and March 4 year averages were averaged to create a winter seasonal emissivity. The 4 year period 2003–2006 was chosen because this period represents consistent processing of the MODIS version 4.0 Day-Night Land Surface Temperature and Emissivity algorithm (later algorithm versions are inconsistent with version 4.0) [*Borbas and Ruston*, 2010]. At each grid cell in the UWIREMIS 0.05° grid, the high spectral resolution UWIREMIS (416 spectral points) was convolved with the ASTER spectral response function for four ASTER infrared channels at 8.7, 9.1, 10.6 and 11.3 μm. The 1 km spatial grid of NAALSED was then scaled to the 0.05° grid of UWIREMIS. Differences between UWIREMIS and NAALSED were found for each grid cell and averaged for the North American domain for the four ASTER channels.

4. Results

4.1. Comparison of CRTM Simulations to Satellite Observations

[27] Differences between SEVIRI brightness temperature observations and CRTM brightness temperature simulations for the infrared surface-sensing channels are discussed. Maps of differences (observations minus simulations) for three of the SEVIRI channels (3.9, 8.7, and 10.8 μm) are depicted in Figure 6. The 12.0 μm channel is not shown in Figure 6, because the difference magnitudes and features are very similar to the 10.8 μm channel. Figure 6 (left) represents CRTM run with NPOESS emissivity, and Figure 6 (right) represents CRTM run with UWIREMIS emissivity. Table 2 shows bias (mean difference) and RMSE for each SEVIRI channel for the full-disk view for observation minus simulation differences, where simulations were run with NPOESS and UWIREMIS.

[28] Figure 6 at 3.9 μm shows that brightness temperature differences over some areas (central Algeria, northern Congo) appear to be improved in the left-hand image compared to the right-hand image, but other areas (northern Niger and Chad) are distinctly worse. However, both emissivity and surface temperature contribute to top-of-atmosphere brightness temperature simulations, so unless the surface temperature is known to be accurate, the effect of either emissivity or surface temperature is difficult to separate. Indeed, the region of high positive values in northern Niger and Chad (central Sahara) can be explained by a low surface temperature bias in the ECMWF analysis fields input into CRTM (so simulated brightness temperatures are correspondingly too low compared to observa-

Table 2. Brightness Temperature Bias and RMSE of SEVIRI Observations Minus CRTM Simulations for Infrared Surface-Sensing SEVIRI Channels, Using the NPOESS and UWIREMIS Emissivity Data Sets as Surface Input to CRTM for 30 May 2010 at 0000 UTC[a]

Channel (μm)	NPOESS		UWIREMIS	
	Bias (K)	RMSE (K)	Bias (K)	RMSE (K)
3.9	0.63	2.16	0.57	2.18
8.7	−2.55	3.82	−0.85	2.13
10.8	−0.67	2.00	−0.56	2.03
12.0	−0.56	1.91	−0.31	1.94

[a]Land and cloud-free pixels only. N = 2,297,929.

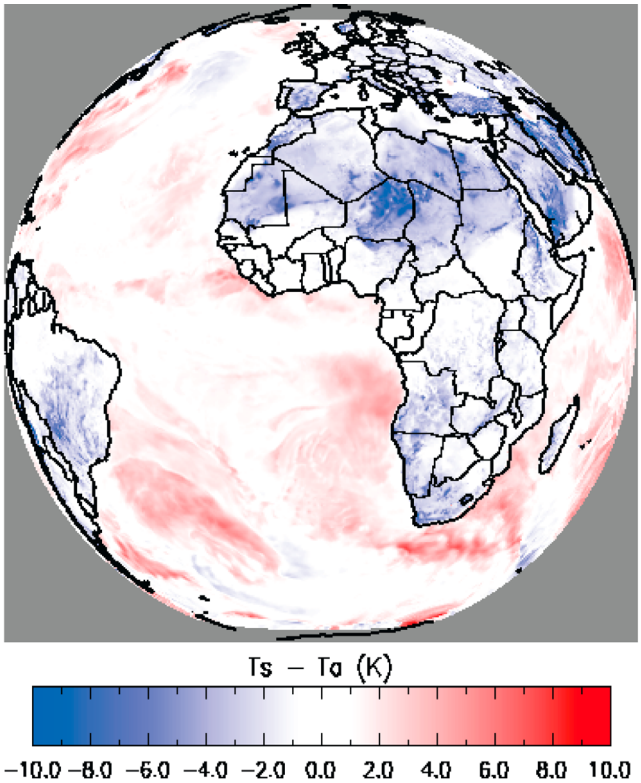

Figure 7. Temperature difference (K) between surface temperature (T_s) analysis and lowest layer air temperature (T_a) analysis at 15 m above the surface, indicating regions of biased surface temperature for ECMWF analysis fields of 30 May 2010 at cycle time 0000 UTC.

tions). The low surface temperature bias is evidenced by comparing the surface temperature analysis to the lowest air temperature in the air temperature profile analysis. Figure 7 shows that the surface temperature can be 8 K lower than the lowest air layer temperature at about 15 m above the surface in certain regions. Such a large difference (colder surface temperature than air temperature) cannot be explained by typical temperature differences associated with temperature inversions, implying error in the surface temperature analysis. Given a biased surface temperature, it is unknown which emissivity is more accurate. If UWIREMIS is correct in the central Sahara, then an incorrectly high NPOESS is compensating for the low surface temperature bias (right 3.9 μm image in Figure 6). Conversely, if NPOESS is correct in the central Sahara, then an incorrectly low UWIREMIS is contributing to the low brightness temperatures and resulting in the high positive difference (left 3.9 μm image in Figure 6). It is not possible to know if one of the two emissivities is more accurate.

[29] Table 2 for 3.9 μm shows a slightly smaller brightness temperature bias with UWIREMIS than NPOESS. However, the small improvement is likely due to better balancing of positive and negative differences (overall creating a smaller bias) and not a real improvement in brightness temperature simulations when using UWIREMIS. RMSE is nearly the same.

[30] Figure 6 at 8.7 μm shows great improvement when using UWIREMIS over NPOESS. The simulations with NPOESS show a broad field of negative values (high simulations compared to observations) over the bare ground surface of the Sahara Desert, indicating that emissivity is too high. These negative values are reduced when using UWIREMIS. As seen in Figure 2, the NPOESS emissivity is entirely lacking the spectral signature of bare ground surfaces in the 8–10 μm region. The advantage of UWIREMIS is that it realistically represents the low-emissivity quartz *reststrahlen* feature common to bare surfaces at these wavelengths. With lower emissivity at the 8.7 μm wavelength, the simulations are also lower which more closely matches the observations (with the exception of northern Niger and Chad owing to the low surface temperature bias, as discussed above). Table 2 shows the improvement in brightness temperature bias and RMSE when using UWIREMIS. The very large negative bias of −2.55 K for the 8.7 μm channel for NPOESS indicates that NPOESS emissivity is too high (simulations higher than observations). This negative bias is substantially improved with the use of lower emissivity in UWIREMIS. RMSE is also substantially improved, exceeding CRTM's RMSE sensitivity to uncertainty in its air temperature, water vapor, or surface temperature inputs (Table 1).

[31] Figure 6 at 10.8 μm shows broad similarity in brightness temperature differences when using NPOESS or UWIREMIS in CRTM. The region in northern Niger and Chad shows slightly more positive differences when using UWIREMIS than NPOESS. Similar to the 3.9 μm case, it is unknown if either the NPOESS emissivity or UWIREMIS is more accurate, owing to the surface temperature bias in this region. Table 2 shows a slight improvement in brightness temperature bias when using UWIREMIS, but again, this is likely due to a better balance of positive and negative differences and not an overall improvement in brightness temperature. RMSE is nearly the same.

[32] Table 2 for 12.0 μm shows a slight improvement in brightness temperature bias with UWIREMIS than NPOESS, but since the difference magnitudes and features are similar to 10.8 μm, the reason for the smaller bias may also be due to better balancing of positive and negative differences.

4.2. Intercomparison With NAALSED

[33] Table 3 shows the results of mean difference between UWIREMIS and NAALSED (calculated as UWIREMIS minus NAALSED) by ASTER channel for both the summer

Table 3. Emissivity Bias and RMSE of UWIREMIS Minus NAALSED for Four ASTER Infrared Channels in Summer and Winter Seasons

	8.7 μm	9.1 μm	10.6 μm	11.3 μm	Mean $\lvert\varepsilon\rvert$[a]
		Summer, N = 341,853			
Bias (K)	0.003	0.007	−0.004	0.001	0.004
RMSE (K)	0.015	0.018	0.007	0.006	
		Winter, N = 251,351			
Bias (K)	−0.008	−0.007	−0.007	−0.004	0.007
RMSE (K)	0.014	0.015	0.009	0.007	

[a]Mean $\lvert\varepsilon\rvert$ represents the mean of the absolute value of all channel biases.

and winter seasons. Bias is very small, ranging from −0.008 to 0.007. RMSE is also small, ranging from 0.006 to 0.018, with the 10.6 and 11.3 μm channels exhibiting smaller RMSE than the other ASTER channels. Summertime bias is positive, meaning that UWIREMIS emissivity is higher than NAALSED (except for the 10.6 μm channel), whereas wintertime bias is negative, meaning that UWIREMIS emissivity is smaller than NAALSED.

5. Discussion

[34] Knowledge of the spectral variation of emissivity is necessary for operational data assimilation systems in order to assimilate the channels of many multispectral and hyperspectral instruments into NWP models. Broadband emissivity and emissivity retrieved at a satellite's channels do not offer sufficient knowledge of emissivity across the spectrum. Because of the nonlinear spectral shape of emissivity for many materials, particularly at infrared wavelengths, the use of emissivity retrieved at a satellite's channels does not allow interpolation of emissivity to determine another instrument's channel emissivity. A full emissivity spectrum at high enough spectral resolution is needed for satellite data assimilation activities involving the growing number of available satellite instruments. The UWIREMIS offers such an emissivity database for satellite data assimilation activities.

[35] Of the four surface-sensing channels used in this evaluation, the one exhibiting improvement when using UWIREMIS over NPOESS is the 8.7 μm channel. This is a result of UWIREMIS realistically characterizing bare ground and desert emissivity in this portion of the spectrum; whereas NPOESS does not represent bare ground emissivity correctly.

[36] For the other channels at 3.9, 10.8 and 12.0 μm, surface temperature bias prevents the assessment of emissivity accuracy of either NPOESS or UWIREMIS at these wavelengths. The effects of surface temperature and emissivity are difficult to separate in the calculation of brightness temperature, so use of observation-simulation brightness temperature differences requires that surface temperatures be accurate in order to assess emissivity. An accurate surface temperature was less of a factor for the 8.7 μm channel because the emissivity error in NPOESS (for bare ground surfaces) substantially outweighed the error in surface temperature, making the improvement in UWIREMIS obvious.

[37] CRTM radiative transfer biases are presumed to be small, given earlier studies, for example, those of *Liang et al.* [2009], showing excellent accuracy of CRTM over ocean for surface-sensing channels of the Advanced Very High Resolution Radiometer (simulation minus observation bias of 0.2 K and 0.35 K for the 3.7 and 11/12 μm channels, respectively). Therefore, if CRTM biases over ocean are small, then biases over land are more likely due to biased inputs such as land surface temperature, atmospheric profiles, and surface emissivity. The treatment of aerosols and BRDF effects over land also need investigation and improvement.

[38] For radiative transfer modeling and data assimilation activities, the ideal surface emissivity is one that represents the field of view of the instrument being simulated. Since the surface characteristics within a field of view may be highly variable, it is necessary to determine the emissivity "seen" by the instrument. To achieve an emissivity value that is spatially relevant, it is necessary to perform spatial scaling studies with accurate high spatial resolution emissivity data sets. In this regard, NAALSED is ideal for spatial scaling studies of emissivity because of its accuracy and high spatial resolution.

[39] The intercomparison of UWIREMIS with NAALSED allows an estimation of UWIREMIS's accuracy. The mean absolute difference for the four ASTER channels (mean of absolute value of the four channels' biases) is 0.004 for the summer and 0.007 for the winter (Table 3), which is well within NAALSED's own bias of 0.016 against in situ measurements. Thus, the UWIREMIS is verified against NAALSED within NAALSED's own validation, suggesting UWIREMIS is an accurate emissivity data set for the NAALSED spatial domain and the spectral region of the ASTER channels.

[40] Other areas are still in need of improvement in order to have accurate emissivities for the surface contribution to radiative transfer models: the effect of soil moisture and snow on emissivity, emissivity dependence on viewing angle [*Ruston et al.*, 2008], and BRDF effects for land surface. *Hulley et al.* [2010] found positive correlation between rainfall events and increased satellite-derived land surface emissivity estimates. This result suggests that the temporal dynamics of soil-moisture influences on emissivity will need investigation to understand the time scales involved. While monthly averaged emissivity data sets capture emissivity variation due to seasonal changes, the observed effect of soil moisture, which varies ephemerally, implies that these short-term changes will require emissivity data sets on temporal scales shorter than one month.

6. Conclusion

[41] Use of emissivity to supply radiative transfer models with surface conditions has been improving in recent years. In the past, radiative transfer models typically employed a single value for emissivity for all surfaces, for example, 0.98. This has given way to spectral emissivity data sets for surface classes based on surface classification schemes [*Snyder et al.*, 1998]. In turn, such generalizations of emissivity by surface class are giving way to high spatial and high spectral resolution data sets derived from satellite measurements. While these satellite-derived data sets have some limitations due to algorithm retrieval performance, the high spatial resolution has potential to represent the high variability of land surface emissivity on small spatial scales. In addition, the high spectral resolution is needed in data assimilation activities for assimilating the channels of the many multispectral and hyperspectral sensors now available.

[42] In this study, we evaluated UWIREMIS in CRTM and compared CRTM brightness temperature simulation results with SEVIRI brightness temperature observations for one full-disk SEVIRI view on 30 May 2010 at 0000 UTC. We found that UWIREMIS emissivity offers substantial improvement for bare ground and desert regions in the 8–10 μm region where bare ground surfaces typically have very low emissivity. Surface temperature biases exist in the ECMWF analysis inputs to CRTM for the time period of this study and need to be considered in combination with emissivity bias. Since the calculation of brightness temper-

ature requires both surface temperature and emissivity, we do not draw a conclusion for the 3.9, 10.8 and 12.0 μm channels about the accuracy of NPOESS or UWIREMIS given the biased surface temperature. This study points to the importance of using accurate surface temperatures for the evaluation of emissivity accuracy when comparing calculated brightness temperature with observed brightness temperatures.

[43] Nevertheless, we assessed UWIREMIS's accuracy against NAALSED and found UWIREMIS to be accurate within NAALSED's own in situ validation. This suggests UWIREMIS to be accurate for the NAALSED spatial domain and for spectral regions near the ASTER channels. These are encouraging results for UWIREMIS.

[44] For radiative transfer applications, high spatial resolution emissivity data sets are needed to capture the small-scale variation of emissivity over land surface, and high spectral resolution emissivity data sets are needed for data assimilation of channels from the many multispectral and hyperspectral sensors now available. UWIREMIS combines both requirements into one data set, so it is well suited for the infrared surface emissivity contribution to radiative transfer models. For some spectral regions such as the 8–10 μm region, UWIREMIS excels at improving top-of-atmosphere satellite simulations for bare ground surfaces compared to the CRTM's existing emissivity data set. Further study will be needed to assess UWIREMIS at other spectral regions and other types of surfaces.

[45] **Acknowledgments.** The authors thank Yunyue Yu, Eva Borbas, Ben Ruston, Andrew Collard, Weizhong Zheng, and Paul van Delst for helpful discussions. We thank the following organizations for making the UWIREMIS, NAALSED, and SEVIRI data available, respectively: University of Wisconsin Cooperative Institute for Meteorological Satellite Studies, Jet Propulsion Laboratory, and EUMETSAT. This work was supported by the Joint Center for Satellite Data Assimilation. The views, opinions, and findings contained in this report are those of the authors and should not be construed as an official NOAA or U.S. Government position, policy, or decision.

References

Aminou, D. M. A., B. Jacquet, and F. Pasternak (1997), Characteristics of the Meteosat Second Generation radiometer/imager: SEVIRI, *Proc. SPIE Int. Soc. Opt. Eng.*, *3221*, 19–31, doi:10.1117/12.298084.

Baldridge, A. M., S. J. Hook, C. I. Grove, and G. Rivera (2009), The ASTER spectral library version 2.0, *Remote Sens. Environ.*, *113*, 711–715, doi:10.1016/j.rse.2008.11.007.

Borbas, E. E., and B. C. Ruston (2010), The RTTOV UWiremis IR land surface emissivity module, *Mission Rep. NWPSAF-MO-VS-042*, Numer. Weather Predict. Satell. Appl. Facil., Eur. Organ. for the Exploit. of Meteorol. Satell., Met Off., Exeter, U. K.

Borbas, E. E., R. O. Knuteson, S. W. Seemann, E. Weisz, L. Moy, and H.-L. Huang (2007), A high spectral resolution global land surface infrared emissivity database, paper presented at the Joint 2007 EUMETSAT Meteorological Satellite Conference and the 15th Satellite Meteorology and Oceanography Conference, Eur. Organ. for the Exploit. of Meteorol. Satell., Amsterdam.

Chen, Y., Y. Han, P. Van Delst, and F. Weng (2010), On water vapor Jacobian in fast radiative transfer model, *J. Geophys. Res.*, *115*, D12303, doi:10.1029/2009JD013379.

Collard, A. D. (2009), Prospects for IASI, CrIS and AIRS in the UKVD, *Forecasting R&D Tech. Rep. 539*, Met Off., Exeter, U. K.

Dorman, J. L., and P. J. Sellers (1989), A global climatology of albedo, roughness length and stomatal resistance for atmospheric general circulation models as represented by the Simple Biosphere model (SiB), *J. Appl. Meteorol.*, *28*, 833–855, doi:10.1175/1520-0450(1989)028<0833:AGCOAR>2.0.CO;2.

Ek, M. B., K. E. Mitchell, Y. Lin, E. Rogers, P. Grunmann, V. Koren, G. Gayno, and J. D. Tarpley (2003), Implementation of Noah land surface model advances in the National Centers for Environmental Prediction operational mesoscale Eta model, *J. Geophys. Res.*, *108*(D22), 8851, doi:10.1029/2002JD003296.

Friedl, M. A., et al. (2002), Global land cover mapping from MODIS: Algorithms and early results, *Remote Sens. Environ.*, *83*, 287–302, doi:10.1016/S0034-4257(02)00078-0.

Gillespie, A., S. Rokugawa, T. Matsunaga, J. S. Cothern, S. Hook, and A. B. Kahle (1998), A temperature and emissivity separation algorithm for Advanced Spaceborne Thermal Emission and Reflection Radiometer (ASTER) images, *IEEE Trans. Geosci. Remote Sens.*, *36*(4), 1113–1126, doi:10.1109/36.700995.

Han, Y., P. van Delst, Q. Liu, F. Weng, B. Yan, R. Treadon, and J. Derber (2005), JCSDA Community Radiative Transfer Model (CRTM): Version 1, *NOAA Tech. Rep. 122*, Natl. Environ. Satell. Data and Inf. Serv., Silver Spring, Md.

Hulley, G. C., and S. J. Hook (2009), The North American ASTER Land Surface Emissivity Database (NAALSED) version 2.0, *Remote Sens. Environ.*, *113*, 1967–1975, doi:10.1016/j.rse.2009.05.005.

Hulley, G. C., S. J. Hook, and A. M. Baldridge (2008), ASTER land surface emissivity database of California and Nevada, *Geophys. Res. Lett.*, *35*, L13401, doi:10.1029/2008GL034507.

Hulley, G. C., S. J. Hook, and A. M. Baldridge (2009), Validation of the North American ASTER Land Surface Emissivity Database (NAALSED) version 2.0 using pseudo-invariant sand dune sites, *Remote Sens. Environ.*, *113*, 2224–2233, doi:10.1016/j.rse.2009.06.005.

Hulley, G. C., S. J. Hook, and A. M. Baldridge (2010), Investigating the effects of soil moisture on thermal infrared land surface temperature and emissivity using satellite retrievals and laboratory measurements, *Remote Sens. Environ.*, *114*, 1480–1493, doi:10.1016/j.rse.2010.02.002.

Liang, X., A. Ignatov, and Y. Kihai (2009), Implementation of the Community Radiative Transfer Model (CRTM) in Advanced Clear-Sky Processor for Oceans (ACSPO) and validation against nighttime AVHRR radiances, *J. Geophys. Res.*, *114*, D06112, doi:10.1029/2008JD010960.

Lillesand, T. M., R. W. Kiefer, and J. W. Chipman (2004), *Remote Sensing and Image Interpretation*, 5th ed., John Wiley, New York.

Liu, Q., and F. Weng (2006), Radiance assimilation in studying Hurricane Katrina, *Geophys. Res. Lett.*, *33*, L22811, doi:10.1029/2006GL027543.

Mira, M., E. Valor, R. Boluda, V. Caselles, and C. Coll (2007), Influence of soil water content on the thermal infrared emissivity of bare soils: Implication for land surface temperature determination, *J. Geophys. Res.*, *112*, F04003, doi:10.1029/2007JF000749.

Persson, A., and F. Grazzini (2007), User Guide to ECMWF Forecast Products, Version 4.0, *Meteorol. Bull. M3.2*, Eur. Cent. for Medium-Range Weather Forecasts, Reading, U. K.

Ruston, B., F. Weng, and B. Yan (2008), Use of one-dimensional variational retrieval to diagnose estimates of infrared and microwave surface emissivity over land for ATOVS sounding instruments, *IEEE Trans. Geosci. Remote Sens.*, *46*(2), 393–402, doi:10.1109/TGRS.2007.910219.

Salisbury, J. W., and D. M. D'Aria (1992), Emissivity of terrestrial materials in the 8–14 μm atmospheric window, *Remote Sens. Environ.*, *42*, 83–106, doi:10.1016/0034-4257(92)90092-X.

Salisbury, J. W., A. Wald, and D. M. D'Aria (1994), Thermal-infrared remote sensing and Kirchhoff's law: 1. Laboratory measurements, *J. Geophys. Res.*, *99*, 11,897–11,911, doi:10.1029/93JB03600.

Seemann, S. W., E. E. Borbas, R. O. Knuteson, G. R. Stephenson, and H.-L. Huang (2008), Development of a global infrared land surface emissivity database for application to clear sky sounding retrievals from multi-spectral satellite radiance measurements, *J. Appl. Meteorol. Climatol.*, *47*, 108–123, doi:10.1175/2007JAMC1590.1.

Snyder, W. C., Z. Wan, Y. Zhang, and Y.-Z. Feng (1998), Classification-based emissivity for land surface temperature measurement from space, *Int. J. Remote Sens.*, *19*(14), 2753–2774, doi:10.1080/014311698214497.

Wan, Z., and Z.-L. Li (1997), A physics-based algorithm for retrieving land-surface emissivity and temperature from EOS/MODIS data, *IEEE Trans. Geosci. Remote Sens.*, *35*(4), 980–996, doi:10.1109/36.602541.

Yu, Y., J. L. Privette, and A. C. Pinheiro (2008), Evaluation of split-window land surface temperature algorithms for generating climate data records, *IEEE Trans. Geosci. Remote Sens.*, *46*(1), 179–192, doi:10.1109/TGRS.2007.909097.

Zhou, L., R. E. Dickinson, Y. Tian, M. Jin, K. Ogawa, H. Yu, and T. Schmugge (2003), A sensitivity study of climate and energy balance simulations with use of satellite-derived emissivity data over Northern Africa and the Arabian Peninsula, *J. Geophys. Res.*, *108*(D24), 4795, doi:10.1029/2003JD004083.

Y. Han, Q. Liu, R. L. Vogel, and F. Weng, Center for Satellite Applications and Research, NOAA, NESDIS, 5200 Auth Rd., Camp Springs, MD 20746, USA. (Ronald.Vogel@noaa.gov)